

Experimental and theoretical contributions to the determination of optical properties of synthetic paramelaconite

J.F. Pierson^{a,*}, E. Duverger^b, O. Banakh^c

^aLaboratoire de Science et Génie des Surfaces (UMR CNRS 7570), Ecole des Mines, Parc de Saurupt, F-54042 Nancy Cedex, France

^bDépartement CREST, Institut FEMTO-ST (UMR CNRS 6174), Université de Franche-Comté, Pôle Universitaire, BP 71427, F-25211 Montbéliard Cedex, France

^cHaute Ecole ARC, Eplatures – Grise 17, CH-2300 La Chaux-de-Fonds, Switzerland

Received 19 October 2006; received in revised form 20 December 2006; accepted 26 December 2006

Available online 10 January 2007

Abstract

Paramelaconite (Cu_4O_3) is a metastable copper oxide that can be barely synthesised in “pure” form. In this study, the reactive magnetron sputtering process was used to deposit Cu_4O_3 films on silicon and glass substrates. The deposited films were characterised by X-ray diffraction (XRD), UV-visible-NIR spectroscopy and spectroscopic ellipsometry. For the first time, the refractive index and the extinction coefficient of Cu_4O_3 were evaluated. The experimental values obtained from spectroscopic ellipsometry were compared to those calculated by a self-consistent approach using the Wien2k code. A very good agreement was found between the two sets of values.

© 2007 Elsevier Inc. All rights reserved.

Keywords: Paramelaconite; Optical properties; Wien2k code

1. Introduction

Paramelaconite (Cu_4O_3) is a metastable copper oxide with a copper-to-oxygen atomic ratio of 1.33, leading to the formula Cu_4O_3 . It crystallises in the tetragonal system (space group: $I4_1/amd$ with $a = 0.5837$ nm and $c = 0.9932$ nm [1]). Although this compound has been discovered in the 1870s as mineral, pure Cu_4O_3 has never been synthesised in bulk or powder form due to the occurrence of both Cu(I) and Cu(II) atoms in this material. Using extraction process of copper oxides with concentrated aqueous ammonia, Morgan et al. [2] have obtained a mixture of Cu_2O , Cu_4O_3 and CuO with the following composition: 27%, 35% and 38%. To overcome the synthesis of pure Cu_4O_3 and to characterise the properties of related oxides, Gomez-Romero et al. [3] have replaced Cu(I) atoms by Ag(I) ones. Using a co-precipitation method, a mixed silver copper oxide ($\text{Ag}_2\text{Cu}_2\text{O}_3$) was synthesised for the first time in 1999.

In order to obtain a pure paramelaconite, other methods have to be considered. Cu_4O_3 films can be deposited by physical vapour deposition, either by sputtering of CuO target with Ar^+ ions [4] or by reactive sputtering of a copper target in O_2 -Ar mixture in RF or DC mode [5]. Since Cu_4O_3 can only be synthesised as thin films, few properties of this phase are available in the literature. von Richthofen et al. [6] showed that Cu_4O_3 can contain up to 2 at% of nitrogen without the structure modification. The thermodynamical properties of Cu_4O_3 films have been measured using differential scanning calorimetry [7]. The Gibbs free energy of formation of Cu_4O_3 is -40 kJ (mol atom)⁻¹, i.e. between that of Cu_2O and CuO (-39.22 and -45.89 kJ (mol atom)⁻¹, respectively) and the heat of formation of paramelaconite, measured by Blobaum et al. is about 21% smaller than that calculated by Moiseev and Vatinin [8]. Medina-Valtierra et al. [9] have deposited Cu_4O_3 films on fibreglass by a chemical vapour deposition process using 2,4-pentanedionate copper (II) as precursor. They reported a low deposition temperature range (about 15 °C) for the synthesis of Cu_4O_3 and studied the reflectance of the films in the visible range.

*Corresponding author. Fax: +33 383 53 47 64.

E-mail address: jean-francois.pierson@mines.inpl-nancy.fr (J.F. Pierson).

Since only a few properties of Cu_4O_3 were reported in the literature, theoretical approaches are very useful to estimate them. In this paper, the optical properties (refractive index and extinction coefficient) of Cu_4O_3 thin films deposited by reactive magnetron sputtering are determined by spectroscopic ellipsometry. A self-consistent calculation approach using the Wien2k code has been carried out to compare experimental and theoretical values.

2. Experimental

2.1. Cu_4O_3 synthesis

Cu_4O_3 films were deposited on glass and silicon (100) substrates by sputtering of a copper target (200 mm diameter and 99.9% purity) in reactive Ar– O_2 mixture. Details on the substrate cleaning procedure and the deposition process can be found elsewhere [10]. As previously discussed [10], the oxygen flow rate, introduced into the deposition chamber, was the critical parameter for the synthesis of the Cu_4O_3 films. In our deposition conditions (RF power applied to the target, argon flow rate, target to substrate distance, total pressure, target diameter, pumping speed), the oxygen flow rate has to be fixed at 5 sccm to allow the deposition of pure Cu_4O_3 films. The use of lower or higher oxygen flow rate induced the formation of cuprite (Cu_2O) or tenorite (CuO) films, respectively.

2.2. Films characterisation

The growth rate of the Cu_4O_3 films deposited on glass substrate was determined by measuring the films thickness by tactile profilometry. The structure of the films deposited on glass substrate was studied by X-ray diffraction (XRD) analysis in $\theta/2\theta$ mode using Cu $K\alpha$ radiation. The mean crystal size was estimated from the full-width at half-maximum (FWHM) of the diffraction peak using the Debye–Scherrer formula, neglecting peak broadening due to intrinsic stress.

The optical transmittance (T) and reflectance (R) were measured by UV-visible-NIR spectroscopy in the 250–2500 nm range. Transmission data were used to estimate the optical band gap (E_g). The refractive index (n) and the extinction coefficient (k) of films deposited on silicon substrate were deduced from spectroscopic ellipsometry at incidence angle of 70° in a 0.75–4.5 eV energy range (1700–270 nm), with a step of 0.02 eV.

2.3. Theoretical method

Self-consistent calculations of total energies and the electronic structure based on the scalar relativistic full-potential (FP) “augmented-plane-wave local orbitals” method (APW+lo) [11] were carried out using the WIEN2k code [12]. This is a very accurate and efficient scheme to solve the Kohn–Sham equations of density

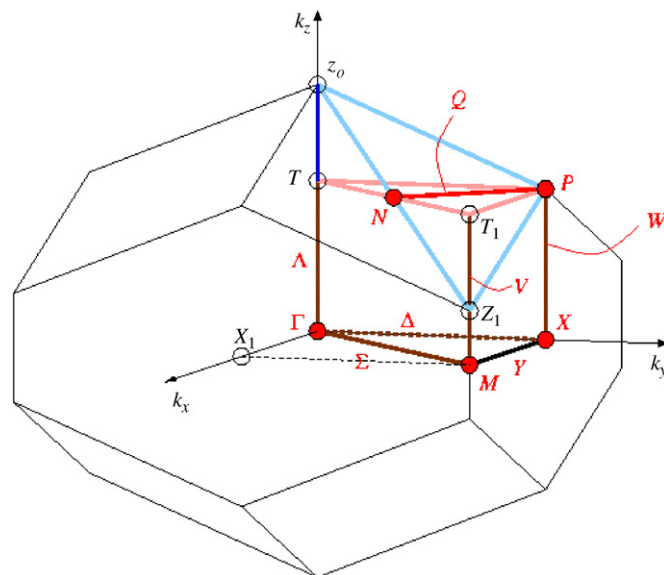


Fig. 1. Schematic representation of the Brillouin zone of the space group $I4_1/amd$, from [13].

functional theory (DFT) in which exchange and correlation effects are treated, for example, by the generalised gradient approximation (GGA) which often leads to better energetic and equilibrium structures than the local density approximation (LDA). The electron density is obtained by summing over all occupied Kohn–Sham orbitals and plays the key role in this formalism. The Cu_4O_3 structure (space group: $I4_1/amd$) contains four inequivalent atoms (two copper and two oxygen). The atomic sphere radii were 1.76 a.u. for Cu and 1.64 a.u. for O. The Brillouin zone (BZ) of the space group $I4_1/amd$ is presented in Fig. 1. The required precision in total energy was achieved by using a large plane-wave (PW) cut-off.

In the linear APW (LAPW) method the relevant convergence parameter is Rk_{\max} , which is defined by the product of the smallest atomic sphere radius times the largest reciprocal lattice vector of the PW basis. We used $Rk_{\max} = 5$ for the structure. A k -point sampling of up to 32,000 points in the full three-dimensional (3D) BZ was used. The k mesh was generated in the irreducible wedge of the BZ on a special point grid which can be used in a modified tetrahedron scheme.

3. Results and discussion

3.1. Structure

The X-ray diffractogram of the copper oxide film deposited with an oxygen flow rate of 5 sccm is displayed in Fig. 2. To confirm the occurrence of the Cu_4O_3 structure in the deposited film, the JCPDS files of Cu_4O_3 and Cu_2O are also presented in Fig. 2 (files 83-1665 and 5-667, respectively). Since the peak located near 64.4° cannot match with Cu_2O , this diffractogram cannot be indexed using the Cu_2O structure. Furthermore, the deposition rate

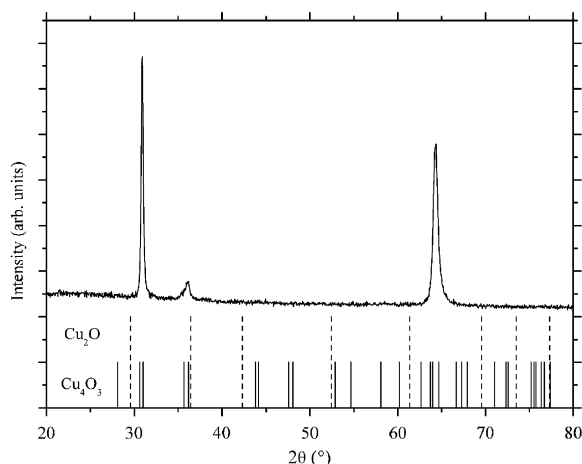


Fig. 2. X-ray diffractogram of a 3.2- μm thick film deposited on glass substrate using 5 sccm of oxygen. The position of diffraction peaks of Cu_2O (JCPDS file 5-667) and Cu_4O_3 (JCPDS file 83-1665) structures are displayed in dash and solid lines, respectively.

of the films synthesised with 5 sccm of oxygen is high ($6.3 \mu\text{m h}^{-1}$) compared to that of CuO films (about $1.2 \mu\text{m h}^{-1}$). Therefore, it can be concluded that the oxygen flow rate of 5 sccm used for sputtering of a copper target leads to the formation of Cu_4O_3 films. The mean crystal size of the Cu_4O_3 films has been estimated from the FWHM of the (200) and (400) diffraction peaks and is about 30 nm. As commonly observed for sputtered films, Cu_4O_3 films exhibit a preferred orientation. Within the deposition conditions used in this study, Cu_4O_3 films exhibit a preferred orientation in the [100] direction [5].

As previously discussed [10], the critical parameter to form Cu_4O_3 thin films by reactive sputtering is the oxygen flow rate. Since Cu_4O_3 contains an oxygen concentration ranging between that of Cu_2O and CuO , the critical oxygen flow rate necessary to form Cu_4O_3 is ranging between those to form Cu_2O and CuO . The oxygen flow rate window to deposit Cu_4O_3 films is very narrow. Within our deposition conditions (power applied to the target, substrate–target distance, total pressure, etc.), this window is narrower than 1 sccm. This result may explain why most of the papers dealing with sputtering of copper in reactive Ar-O_2 mixtures did not report a successful deposition of the Cu_4O_3 coatings [14–17].

3.2. Optical properties

Another way to clearly distinguish Cu_4O_3 from other copper oxides is by studying the optical properties. The optical transmittance of a Cu_4O_3 film is presented in Fig. 3. For comparison, the transmittance of a CuO film with nearly the same thickness is also presented. The absorption edge of the Cu_4O_3 film is shifted about 70 nm to lower wavelength values compared to CuO . As previously discussed [18], the occurrence of this shift indicates that the optical band gap of Cu_4O_3 differs from that of CuO . The optical band gap (E_g) of Cu_4O_3 thin films has been

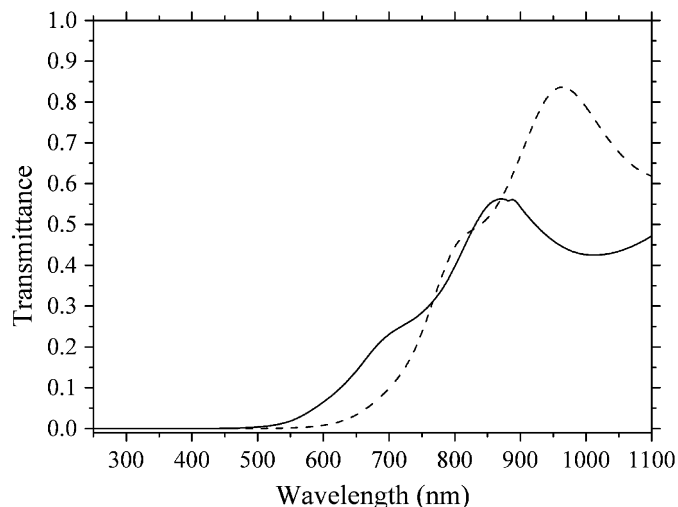


Fig. 3. Optical transmittance of a 0.55- μm thick Cu_4O_3 film (solid line) and a 0.56- μm thick CuO film (dash line) deposited on glass substrates.

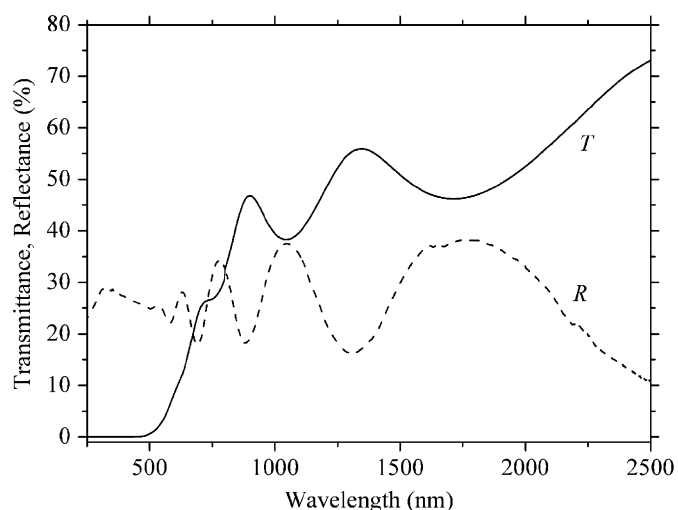


Fig. 4. Transmittance (solid line) and reflectance (dash line) of a 0.55- μm thick Cu_4O_3 film deposited on glass substrate.

estimated assuming Cu_4O_3 as an indirect semiconductor. Using UV-visible transmission measurements, E_g is determined by plotting $(\alpha h\nu)^{0.5}$ versus $h\nu$ and by extrapolating the full line to the abscissa (α denotes the absorption coefficient and $h\nu$ the photon energy). The optical band gap of Cu_4O_3 films is close to 1.34 eV, which is different from those of Cu_2O and CuO . Indeed, these copper oxides are well-known to be direct semiconductors [19,20].

To get more information about the optical properties of paramelaconite, the transmittance and the reflectance have been measured in the 250–2500 nm range (Fig. 4). At low wavelengths ($\lambda < 500$ nm), the Cu_4O_3 transmittance (T) is close to 0, whereas the reflectance (R) is ranging between 25% and 30%. Assuming that the light scattering at the films surface can be neglected, the absorbance (A) is estimated from:

$$A = 1 - T - R. \quad (1)$$

Thus, Cu_4O_3 films exhibit high absorbance (nearly 70%) at low wavelengths. After the absorption edge, the absorbance strongly decreases to become quite constant (nearly 15%) for the wavelength higher than 1500 nm.

Spectroscopic ellipsometry was used to determine refractive index (n) and extinction coefficient (k) (Fig. 5) of the films. In the 0.75–4.5 eV energy range, the Cu_4O_3 refractive index is ranging between 2.24 and 3.10. As previously discussed, no information about the refractive index of Cu_4O_3 is available in the literature while the optical properties of Cu_2O and CuO films are well-known [14,21,22]. Compared to the refractive index of Cu_2O , CuO and mixed $\text{Cu}_2\text{O}+\text{CuO}$ films obtained by Paretta et al. [14], the refractive index of our Cu_4O_3 films shows a less pronounced variation in the 0.75–1.5 eV energy range, proving again that our films deposited by reactive sputtering are not a mixture of different copper oxides. At low photon energy, the k -value of Cu_4O_3 films slightly differs from 0, indicating that Cu_4O_3 may not exhibit dielectric properties contrary to Cu_2O or CuO films [14,22].

3.3. Calculation of optical properties

A deeper understanding of electronic structures can be obtained by studying optical spectra which not only give information about the occupied and unoccupied states, but also about the character of bands. Therefore we have calculated the optical properties for the Cu_4O_3 structure and compared them with available experimental data. Once energies ε_{ck} and functions $|\mathbf{k}\rangle$ for the n bands are obtained self-consistently, the interband contribution to the imaginary part of the dielectric functions $\text{Im } \varepsilon_{\alpha\alpha}(\omega)$ can be calculated by summing transitions from occupied to unoccupied states with fixed k vector over the BZ, weighted with the appropriate matrix element for the probability of the transition. To be specific, the components of $\varepsilon_{\alpha\alpha}(\omega)$ are

given by

$$\text{Im } \varepsilon_{\alpha\beta}(\omega) = \frac{4\pi e^2}{m^2 \omega^2} \sum_{c,v} \int dk \langle c_k | P^\alpha | v_k \rangle \langle v_k | P^\beta | c_k \rangle \delta(\varepsilon_{c_k} - \varepsilon_{v_k} - \omega). \quad (2)$$

Here P is the projection operator and c_k, v_k are linked to the Fermi distribution. The evaluation of the matrix elements in the equation is done over the muffin–tin and interstitial regions, separately. Due to the structure of Cu_4O_3 , the dielectric function is a tensor. By an appropriate choice of the principal axes we can diagonalise it and restrict our considerations to the diagonal matrix elements. We have calculated the two components of the dielectric constants corresponding to the electric field parallel to the crystallographic axes a (100), and c (001), respectively. The real part of the components of the dielectric tensor $\varepsilon_{\alpha\alpha}(\omega)$ is then calculated via the equation:

$$\text{Re } \varepsilon_{\alpha\beta}(\omega) = \delta_{\alpha\beta} + \frac{2}{\pi} P \int_0^\infty \frac{\omega' \text{Im } \varepsilon_{\alpha\beta}(\omega')}{\omega'^2 - \omega^2} d\omega'. \quad (3)$$

Knowledge of both the real and imaginary parts of the dielectric tensor allows the calculation of the optical constants ($n_{\alpha\alpha}$ and $k_{\alpha\alpha}$):

$$n_{\alpha\alpha}(\omega) = \sqrt{\frac{|\varepsilon_{\alpha\alpha}(\omega)| + \text{Re } \varepsilon_{\alpha\alpha}(\omega)}{2}}, \quad (4)$$

$$k_{\alpha\alpha}(\omega) = \sqrt{\frac{|\varepsilon_{\alpha\alpha}(\omega)| - \text{Re } \varepsilon_{\alpha\alpha}(\omega)}{2}}. \quad (5)$$

In this paper, we present the refractive index n and the extinction coefficient k . The calculations yield unbroadened functions. To reproduce the experimental conditions more correctly, it is necessary to broaden the calculated spectra. The exact form of the broadening function is unknown, although comparison with measurements suggests that the broadening usually increases with increasing excitation energy due to the vibration between atoms. Also the instrumental resolution smears out many fine features. To simulate these effects the lifetime broadening was simulated by convoluting the absorptive part of the dielectric function with a Lorentzian, whose FWHM is equal to the energy of the channel in eV. The experimental resolution was simulated by broadening the final spectra with a Gaussian, where FWHM is equal to 2.75 eV).

A deeper understanding of optical properties is important from a fundamental point of view, since the optical characteristics involve not only the occupied and unoccupied parts of the electronic structure but also the character of the bands. As the optical properties of materials originate from interband transitions from occupied to unoccupied bands it is more instructive to turn to the electronic band structure. The calculated band structure (spin up, spin down) of Cu_4O_3 is shown in Fig. 6. From this illustration it clearly appears that Cu_4O_3 is an indirect band gap semiconductor where the band gap is between the Γ and Z . Our value for the direct gap (~ 1.2 eV for spin down)

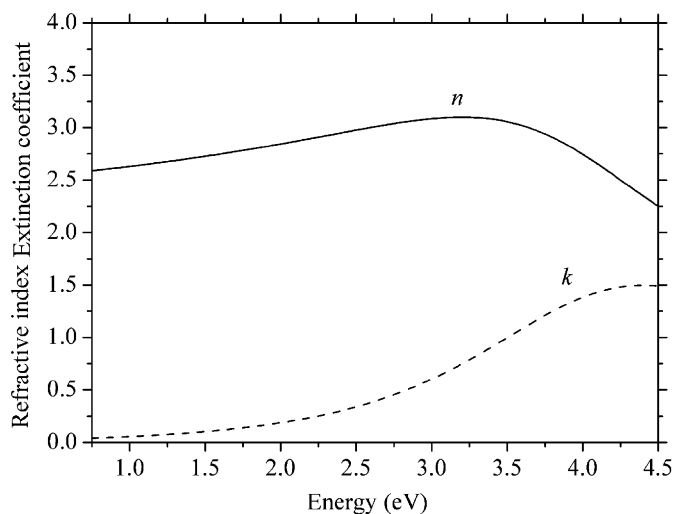


Fig. 5. Refractive index (solid line) and extinction coefficient (dash line) of a 0.55 μm thick Cu_4O_3 film deposited on silicon substrates.

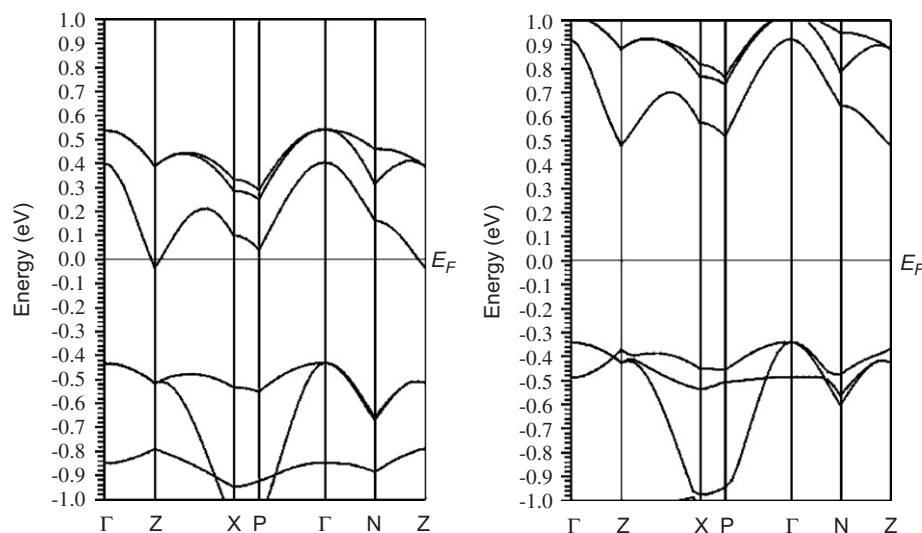


Fig. 6. Calculated band structure of paramelaconite: (a) spin up and (b) spin down.

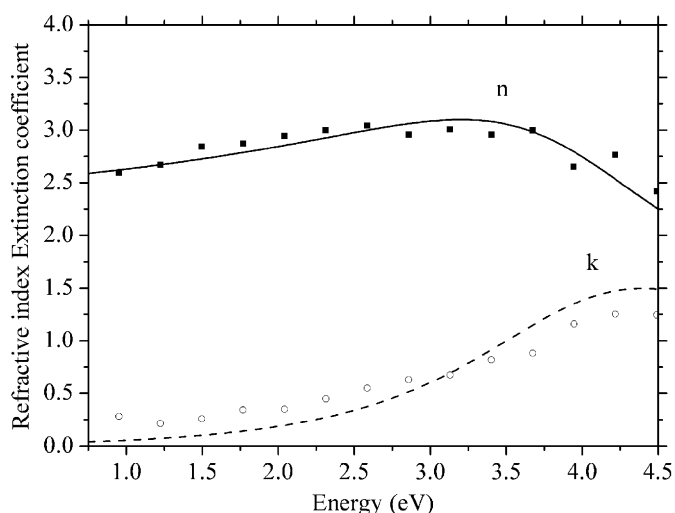


Fig. 7. Comparison between experimental (lines) and calculated (points) refractive index and extinction coefficient values. For experimental measurements, the film was deposited on silicon substrate.

between occupied and empty states at the same location in BZ is too low in comparison with optical measurements assuming Cu_4O_3 as a direct semiconductor (2.47 eV) [10]. This difference between experimental and theoretical values confirms the occurrence of an indirect band gap in the Cu_4O_3 band structure. It should be noted, however, that optical gaps are usually defined at the onset of an increase in spectral intensity in the measured optical variable. The optical anisotropy in this material can be understood from directional-dependent optical dielectric tensor due to the tetragonal symmetry of the lattice. As the linear optical spectra are directly measurable experimentally, we have reported our calculated optical spectra in Fig. 7. Overall our calculated reflectivity spectra are found to be in good qualitative agreement with the experimental spectra.

4. Conclusion

Paramelaconite (Cu_4O_3) films have been deposited by magnetron reactive sputtering on glass and silicon substrates by adjusting the oxygen flow rate in the deposition chamber. XRD clearly shows that the films have a Cu_4O_3 structure and cannot be confused with Cu_2O . Furthermore, the optical transmittance spectrum of Cu_4O_3 films differs from that of CuO films. For the first time, refractive index and extinction coefficient of Cu_4O_3 films have been measured by spectroscopic ellipsometry. The refractive index of the films is between 2.24 and 3.10 in the 0.75–4.5 eV energy range. The extinction coefficient of the films suggests that Cu_4O_3 may not exhibit dielectric properties contrary to Cu_2O and CuO and is a low band gap semiconductor. The Wien2k code has been used to calculate the optical properties of paramelaconite. A good agreement has been found between experimental and theoretical values. Furthermore, the band structure of Cu_4O_3 has been calculated. The results show that Cu_4O_3 is an indirect semiconductor material.

References

- [1] JCPDS Powder Diffraction File 83-1665, International Centre for Diffraction Data, Park Lane, Swarthmore, PA, USA.
- [2] P.E.D. Morgan, D.E. Partin, B.L. Chamberland, M. O'Keeffe, *J. Solid State Chem.* 121 (1996) 33.
- [3] P. Gomez-Romero, E.M. Tejada-Rosales, M. Rosa Palacin, *Angew. Chem. Int. Ed.* 38 (1999) 524.
- [4] J. Li, G. Vizkelethy, P. Revesz, J.W. Mayer, K.N. Tu, *J. Appl. Phys.* 69 (1991) 1020.
- [5] A. Thobor, J.F. Pierson, *Mater. Lett.* 57 (2003) 3676.
- [6] A. von Richthofen, R. Domnick, R. Cremer, D. Neuschütz, *Thin Solid Films* 317 (1998) 282.
- [7] K.J. Blobaum, D. Van Heerden, A.J. Wagner, D.H. Fairbrother, T.P. Weihs, *J. Mater. Res.* 18 (2003) 1535.
- [8] G.K. Moiseev, N.A. Vatolin, *Russ. J. Phys. Chem.* 72 (1998) 1398.

- [9] J. Medina-Valtierra, J. Ramirez-Ortiz, V.M. Arroyo-Rojas, P. Bosch, J.A. de los Reyes, *Thin Solid Films* 405 (2002) 23.
- [10] J.F. Pierson, A. Thobor-Keck, A. Billard, *Appl. Surf. Sci.* 210 (2003) 359.
- [11] G.K.H. Madsen, P. Blaha, K. Schwarz, E. Sjöstedt, L. Nordström, *Phys. Rev. B* 64 (2001) 195134.
- [12] P. Blaha, K. Schwarz, G. K. H. Madsen, D. Kvasnicka, J. Luitz, Computer code WIEN2k, an augmented plane wave plus local orbitals program for calculating crystal properties, University of Technology, Vienna, 2001.
- [13] Bilbao Crystallographic server, <www.cryst.ehu.es>.
- [14] A. Paretta, M.K. Jayaraj, A. Di Nocera, S. Loreti, L. Quercia, A. Agati, *Phys. Stat. Sol. A* 155 (1996) 399.
- [15] S. Ishizuka, T. Maruyama, K. Akimoto, *Jpn. J. Appl. Phys.* 39 (2000) L786.
- [16] S. Ghosh, D.K. Avasthi, P. Shah, V. Ganesan, A. Gupta, D. Sarangi, R. Bhattacharya, W. Assmann, *Vacuum* 57 (2000) 377.
- [17] A.A. Ogwu, E. Bouquerel, O. Ademosu, S. Moh, E. Crossan, F. Placido, *J. Phys. D: Appl. Phys.* 38 (2005) 266.
- [18] J.F. Pierson, D. Wiederkehr, A. Billard, *Thin Solid Films* 478 (2005) 196.
- [19] L. Kleiman, K. Mudnick, *Phys. Rev. B* 21 (1980) 1549.
- [20] W.Y. Ching, Y.-N. Xu, K.W. Wong, *Phys. Rev. B* 40 (1989) 7684.
- [21] T. Mahalingam, J.S.P. Chitre, S. Rajendran, M. Jayachandran, M.J. Chockalingam, *J. Cryst. Growth* 216 (2000) 304.
- [22] B. Balamurugan, B.R. Mehta, *Thin Solid Films* 396 (2001) 90.